Effects of breakup couplings on ^{8}B + ^{58}Ni elastic scattering

J. Lubian,[1,*] T. Correa,[1] E. F. Aguilera,[2] L. F. Canto,[3] A. Gomez-Camacho,[2] E. M. Quiroz,[2] and P. R. S. Gomes[1]

[1]*Instituto de Física, Universidade Federal Fluminense, Av. Litoranea s/n, Gragoaí, 24210-340 Niterói, R. J., Brazil*

[2]*Instituto Nacional de Investigaciones Nucleares, Apartado Postal 18-1027, C. P. 11801 Mexico, D. F., Mexico*

[3]*Instituto de Física, Universidade Federal do Rio de Janeiro, C. P. 68528, 21941-972 Rio de Janeiro, Brazil*

(Received 3 March 2009; revised manuscript received 23 April 2009; published 16 June 2009)

We use the continuum discretized coupled channel (CDCC) method to investigate the effects of breakup coupling on ^{8}B + ^{58}Ni elastic scattering. We evaluate angular distributions at several collision energies and show that our theoretical results are in excellent agreement with the recent data of Aguilera *et al.* [Phys. Rev. C **79**, 021601(R) (2009)]. We show that nuclear excitations of the target have a weak influence on the elastic angular distributions but that the inclusion of continuum-continuum couplings is essential to reproduce the data.

DOI: 10.1103/PhysRevC.79.064605 PACS number(s): 24.10.Eq, 24.10.Ht, 25.70.Bc

I. INTRODUCTION

Nuclear reactions involving weakly bound nuclei have been extensively investigated over the last years [1]. Because of the low breakup threshold, collisions of weakly bound systems have large breakup cross sections. Furthermore, the breakup process affects also the cross sections for other reaction channels, e.g., fusion and elastic scattering [1,2]. Several experiments with stable and unstable weakly bound projectiles have been performed and several theoretical models have been proposed [1].

Nuclear reactions induced by ^{8}B projectiles have attracted particular interest, because the Coulomb dissociation of this nucleus leads to important information for understanding solar neutrino emission. Because ^{8}B is a proton-halo nucleus with a very low breakup threshold ($B = 0.137$ MeV), collisions of ^{8}B with heavy- and medium-mass targets are strongly influenced by Coulomb dissociation. However, the short half-life ($t_{1/2} = 770$ ms) of this nucleus makes the experiments rather difficult. The first measurements of ^{8}B breakup were rather inclusive and led to qualitative information about the breakup process [3]. More recently, Kolata *et al.* [4] provided more exclusive information about ^{8}B breakup, measuring energy spectra for the ^{7}Be fragment produced by ^{8}B breakup, in ^{8}B + ^{58}Ni collisions.

Because the breakup process involves unbound states of the projectile's fragments, the proper theoretical approach for this collision is the coupled channel method including continuum states. For practical purposes it is necessary to approximate the continuum by a finite number of channels. This is achieved by continuum discretization such as in the continuum discretized coupled channel (CDCC) method [5]. Several CDCC calculations have been performed to describe ^{8}B + ^{58}Ni collisions. Nunes and Thompson [6,7] investigated the roles of Coulomb and nuclear interactions in the ^{8}B breakup and also the importance of multistep processes in angular distributions. Tostevin, Nunes, and Thompson [8] performed detailed calculations of energy spectra of the ^{7}Be fragment produced by the breakup process, at several angles. Their results were in very good agreement with the data of Ref. [4]. A semiclassical version of the CDCC method has been developed [9] and used to evaluate the same cross sections studied in Refs. [6–8]. Their results were in good agreement with the full quantum mechanics calculations and with the data of Ref. [4]. Other CDCC studies of the ^{8}B + ^{58}Ni system were performed to derive polarization potentials associated with the breakup channel [10] and to study the influence of breakup on quasielastic barrier distributions [11].

Recently, new data have become available for the ^{8}B + ^{58}Ni system. Aguilera *et al.* [12] measured elastic angular distributions at several collision energies, in the barrier region. So far, no realistic calculation is available for comparison with these new data. In the present work, we perform a theoretical study of the effect of the breakup channel on the elastic angular distributions for the ^{8}B + ^{58}Ni system, using the CDCC method. This article is organized as follows. In Sec. II we discuss the model space used in our CDCC calculations. In Sec. III we present and discuss our results. Finally, in Sec. IV we present our conclusions.

II. CDCC MODEL SPACE

We adopted in our CDCC calculations for the ^{8}B + ^{58}Ni system the same model space as that of Refs. [8] and [10], for which the convergence at energies above the barrier has been checked. Recently [11], the convergence checks have been extended to energies around and below the Coulomb barrier. In this section, we summarize the main features of our CDCC calculations.

The radioactive ^{8}B nucleus is described as an inert ^{7}Be core plus one proton. In the entrance channel, the two fragments are bound, with a separation energy of 0.137 MeV. The remaining projectile's states included in the model space are in the continuum. In the calculations of the coupling matrix elements, the spin of the ^{7}Be core has been neglected, because our ^{7}Be-p interaction is not spin dependent. Thus, the only bound state of the projectile is its $1p_{3/2}$ ground state. The continuum states are approximated by a set of square-integrable bin wave functions. The bins are linear combinations of ^{7}Be + p scattering states, with centroids ε_i at ^{7}Be-p relative energies

*lubian@if.uff.br

in the range $0 < \varepsilon_i < \varepsilon_{\max}$. To guarantee convergence below and above the Coulomb barrier ($V_B = 20.8$ MeV), we used, respectively, $\varepsilon_{\max} = 5$ and 8 MeV. In calculations of coupling matrix-elements involving bin states, the radial integrals were extended up to $R_{\text{bin}} = 60$ fm. For each bin, we considered the values $l = 0, \ldots, 3\hbar$ for the orbital angular momentum associated with the ^{7}Be-p relative motion.

In addition to the intrinsic excitations of the projectile in the continuum, our coupled channel calculations took into account the main excitations of the target, as in Ref. [11]. The corresponding channels are labeled by the value of the target's intrinsic angular momentum I. The wave functions of the relative projectile-target motion were expanded in partial waves, up to $L_{\max} = 1000$. In this way, the wave function with total angular momentum J and z-projection M is schematically written as

$$\Psi^{JM}(\mathbf{R}, \mathbf{r}, \xi) = \sum_i \frac{F_i^J(R)}{R} \mathcal{Y}_i^{JM}(\hat{\mathbf{R}}, \mathbf{r}, \xi). \quad (1)$$

For simplicity of notation, the index i stands for the set of quantum numbers $\{\varepsilon_i l_i j_i I_i, L\}$. In Eq. (1), $\mathbf{r}$ represents the internal coordinates of the projectile, that is, the vector joining the proton and the center of the core; $\mathbf{R}$ is the projectile-target separation vector; $\hat{\mathbf{R}}$ represents its angular degrees of freedom; and ξ stands for the intrinsic coordinates of the target. With the expansion of Eq. (1), one obtains the coupled channel equations

$$\left[T_L + U_{ii}^J(R) - E + \epsilon_i\right] F_i^J(R) = -\sum_j U_{ij}^J(R) F_j^J(R). \quad (2)$$

The index $i = 0$ stands for the elastic channel, where both the projectile and the target are in their ground states ($\varepsilon_0 = 0$, $l_0 = 1$, $j_0 = 3/2$, and $I_0 = 0$). Channels with $i > 0$ are associated with continuum bins and/or an excited state of the ^{58}Ni target. In Eq. (2), ϵ_i stands for the total excitation energy of channel i, $\epsilon_i = \varepsilon_i + e_i$, with e_i representing the target's excitation energy. The coupled equations are solved numerically, up to the matching radius $R = 500$ fm.

The projectile target interaction can be split into two parts, according to the expression

$$V(\mathbf{R}, \mathbf{r}, \xi) = V_{cT}(\mathbf{R}, \mathbf{r}, \xi) + V_{pT}(\mathbf{R}, \mathbf{r}, \xi). \quad (3)$$

The first and the second terms at the right-hand side of Eq. (3) correspond, respectively, to the core-target and the proton-target interactions. The matrix-elements U_{ij}^J in Eq. (2) are given by

$$U_{ij}^J(R) = \int d\hat{\mathbf{R}} d^3\mathbf{r}\, d\xi\ \mathcal{Y}_i^{JM*}(\hat{\mathbf{R}}, \mathbf{r}, \xi) V(\mathbf{R}, \mathbf{r}, \xi) \mathcal{Y}_j^{JM}(\hat{\mathbf{R}}, \mathbf{r}, \xi). \quad (4)$$

The diagonal matrix-elements $U_{ii}^J(R)$ correspond to the optical potentials. In particular, $U_{00}^J(R)$ is the potential in the elastic channel. In our calculations, we take into account off-diagonal matrix-elements between channels with different projectile states or different target states. Couplings between channels where both the projectile and the target are in different states are neglected. To evaluate $U_{ij}^J(R)$, we perform multipole expansions of the interaction and keep up to quadrupole terms.

III. RESULTS AND DISCUSSION

To investigate the reaction mechanisms in ^{8}B + ^{58}Ni scattering, we performed several coupled channel calculations, using the computer code FRESCO [13]. For the proton-target and ^{7}Be-p interactions, we adopted, respectively, the potentials of Becchetti and Greenless [14] and Esbensen and Bertch [15]. In the latter case, the same potential was used for all values of the orbital angular momentum of the ^{7}Be-p relative motion. Excitations of the ^{7}Be core were not taken into account. In some of our calculations we included the channels corresponding to the first 2_1^+ one-phonon excited state of the ^{58}Ni target as well as the triplet of two-phonon states (2_2^+, 4_1^+, and 0_2^+). The deformation parameter was taken from Ref. [16] and we assumed the same shape for proton and neutron densities. For the ^{7}Be-target interaction, we adopted the potential of Moroz *et al.* [17], obtained from ^{7}Li + ^{58}Ni elastic scattering data. Although this potential has been derived from the ^{7}Li projectile, it is the mirror nucleus of ^{7}Be, with nearly the same mass and similar nuclear structure properties.

In Fig. 1, we compare experimental angular distributions at several collision energies with the results of our CDCC model, within different approximations. The data are from Ref. [12]. In the simplest calculation (long-dashed line), we have reduced the coupled channel equations to a single-channel problem, setting all couplings equal to zero. In this case the Hamiltonian contains only the potential corresponding to the diagonal matrix-element of Eq. (4) evaluated in the entrance channel, $U_{00}^J(R)$. Although the results are consistent

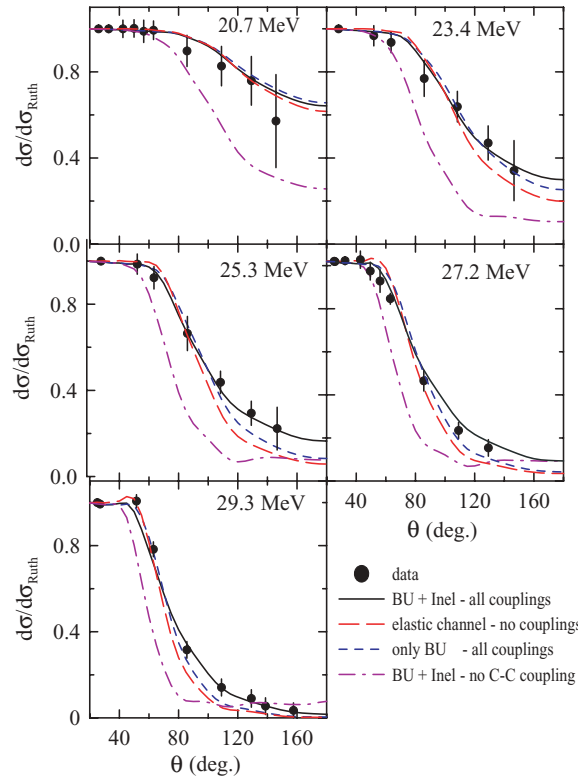

FIG. 1. (Color online) Angular distributions predicted by several CDCC calculations, in comparison with the data of Ref. [12]. For details, see the text.

with the data at the lowest collision energies, $E_{\rm lab} = 20.7$ and 23.4 MeV, they are well below the data at large angles for the collision energies $E_{\rm lab} = 25.3, 27.2$, and 29.3 MeV. The solid line represents the results of our best CDCC calculation. It includes channels corresponding to all bin states (breakup) and the inelastic target excitations, as well as all couplings among these channels. The results are in excellent agreement with the data of Ref. [12] for the five collision energies and in the whole angular region covered in the experiment.

Now we investigate the importance of inelastic excitations and of the couplings among the bin states. A CDCC calculation including all bins and continuum-continuum couplings, but leaving out inelastic excitations of the target, was made. The results are indicated by the short-dashed line. Although they still underestimate the experimental results for the highest collision energies at large angles, they are clearly better than the ones in the no-coupling case. The remaining difference between calculations and the data should be attributed to other reaction mechanisms, like inelastic excitation of the core [18] and of the target, although this effect does not seem to be very important. This result is consistent with the experiment of Ref. [12], where no significant inelastic excitations were found. Nevertheless, inelastic excitations of the target have an appreciable influence on the quasielastic barrier distribution for this system [10]. The fourth calculation (dot-dashed line) takes into account all bin states of the projectile and also the inelastic excitations of the target. However, the calculations leave out continuum-continuum couplings. This is by far the worst calculation. The calculations are well below the experimental angular distribution for all collision energies, even at small angles. This conclusion is consistent with the results of other CDCC calculations. Nunes and Thompson [7] investigated the effects of multistep processes in the angular distributions of the center of mass of the ^{8}B projectile in breakup reactions on a ^{58}Ni target. They found that multistep processes lead to a strong suppression of the breakup cross section at large angles. Therefore, the absorption of the incident wave is reduced. This leads to an increase of the elastic cross section, as found in the present work. A conclusion along these lines has also been reached in CDCC calculations of fusion cross sections [19], where continuum-continuum couplings have been shown to lead to a strong suppression of fusion cross sections at near-barrier energies.

It is frequently argued that exclusive experiments with great accuracy are necessary to assess the effects of the breakup process on the cross sections for the various reaction channels. In principle, this claim is correct. However, some relevant information about the physical processes involved in the collision can be extracted even from experiments with radioactive beams, with large error bars. This information can be used to derive polarizations associated with breakup coupling [20] and to develop studies along the lines of the present work.

The use of ^{7}Be-target and p-target potentials determined from elastic scattering data, together with the coupled channel method, may lead to some double counting of inelastic excitation. To assess the importance of these effects, we ran a few tests replacing these interactions by double folding potential for the real part and standard fusion absorption,

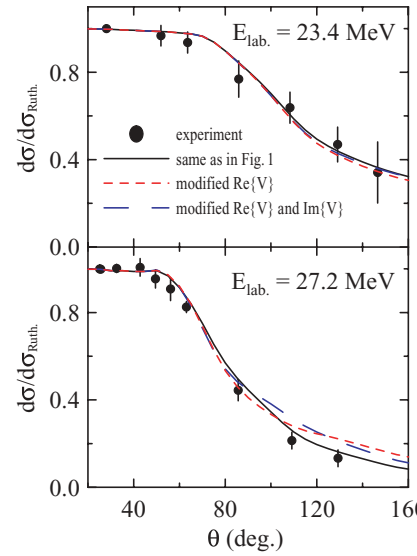

FIG. 2. (Color online) Angular distributions for different choices of the interactions. The solid lines were obtained with the ^{7}Be-target and p-target potentials described in the text. For the short- and long-dashed lines, we replaced the imaginary part of the diagonal matrix-elements of the interaction by a Woods-Saxon function, representing strong fusion absorption. For the short-dashed line, we replaced also the real part by a double-folding interaction.

parametrized by Woods-Saxon functions. We found that the results at low energy are nearly the same. At higher energies, there are some differences at large backward angles. This is illustrated in Fig. 2, in the cases of two collision energies, one below and one above the barrier.

In the CDCC calculations of Fig. 1, the entrance channel and the channels associated with the bin states of the target are coupled among themselves through the action of the potential of Eq. (3), which contains both Coulomb and nuclear contributions. Now we investigate the importance of each of these contributions and the interference between them. For this purpose, we perform CDCC calculations switching off each of these interactions and comparing the results with the ones obtained with the full couplings. This procedure is illustrated in Fig. 3, for the elastic angular distribution at $E_{\rm lab.} = 20.7$ MeV. The short-dashed line corresponds to the CDCC calculation with pure Coulomb breakup, the long-dashed line contains pure nuclear breakup, and the thick solid line represents the CDCC calculations with full breakup couplings. In the three curves both the nuclear and Coulomb contributions to the couplings between the elastic channels and the channels associated with inelastic excitations of the target are taken into account. For comparison, we show also the data of Ref. [12] and the results of a single-channel calculation, switching off the couplings with any bin state or inelastic excitation (thin solid line). We first notice that the angular distribution (normalized with respect to the Rutherford cross section) obtained with purely Coulomb breakup coupling is slightly higher than the one where the couplings to all the bin states are switched off. This suggests that the polarization potential associated with Coulomb breakup is repulsive in the barrier region. Note that the collision

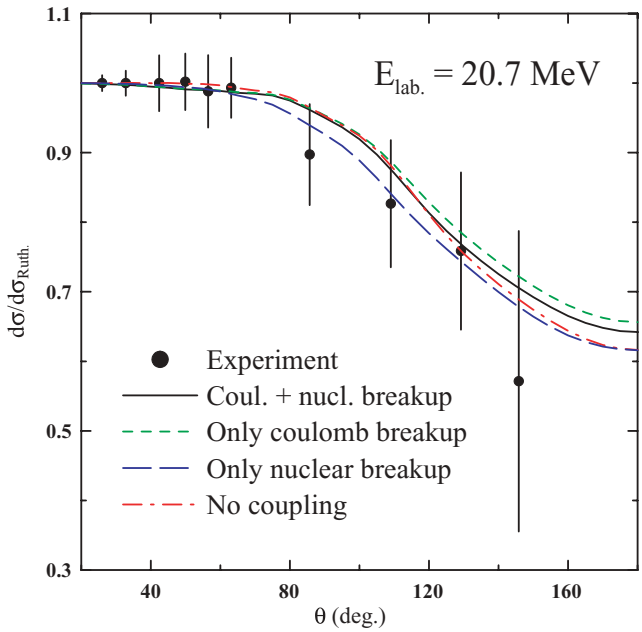

FIG. 3. (Color online) Effects of Coulomb and nuclear breakup on the elastic angular distribution at $E_{lab.} = 20.7$ MeV. The dash-dotted line are results of an optical model calculation, with all couplings switched off. The remaining curves are results of different CDCC calculations. They include the relevant couplings with bound excited channels but they treat differently the couplings with continuum states. The solid line represents our best calculation, in which both Coulomb and nuclear couplings are taken into account. The short-dashed and the long-dashed lines represent, respectively, results of CDCC calculations considering exclusively Coulomb and nuclear breakup. For comparison, we show also the data from Ref. [12].

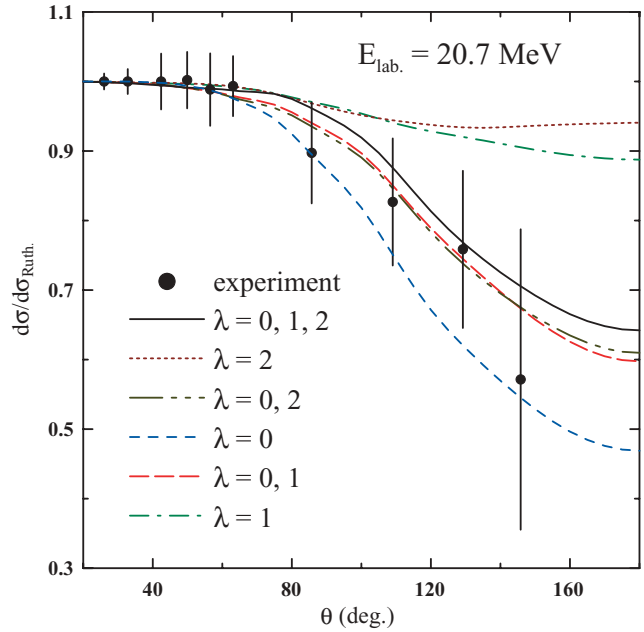

FIG. 4. (Color online) Contribution from each term in the multipole expansion of the interacting potentials. Different CDCC calculations were performed, considering (i) monopole, (ii) dipole, (iii) monopole + dipole, (iv) quadrupole, and (v) all multipoles. The lines corresponding to the calculations are indicated inside the figure frame. For details, see the text.

energy $E_{lab.} = 20.7$ MeV ($\equiv E_{c.m.} = 18.2$ MeV) is already below the barrier of the bare potential, $V_B = 20.8$ MeV. The addition of a repulsive polarization term increases the height of the barrier and this leads to a larger rainbow angle and reduces the fusion absorption. However, the results for purely nuclear breakup coupling fall slightly below the results of the single-channel calculation. When both nuclear and Coulomb breakup couplings are taken into account, there is a destructive interference between the two amplitudes and the angular distribution lies slightly above the no-coupling results. Although our discussion has been based on the data at $E_{lab.} = 20.7$ MeV, the conclusions for the other energies are qualitatively similar.

We now investigate the contribution of each term in the multipole expansion of the coupling interaction of Eq. (3). We have checked that multipoles higher than $\lambda = 2$ have negligible effects on the angular distributions. Thus, our study is restricted to the role of the monopole, dipole, and quadrupole terms of the expansion. In Fig. 4 we show the results of several CDCC calculations. The solid line corresponds to our best calculation, which includes all relevant multipoles. The short-dashed and the dot-dashed lines were obtained, respectively, with only the monopole and the dipole term. In this case, only transitions between breakup states are accounted for (see details about inelastic excitations below). It is clear that the monopole and dipole terms lead, respectively, to attractive and repulsive polarization potentials. When these two multipolarities are simultaneously included in the calculation (long-dashed line), the results fall slightly below the solid line, showing that they interfere destructively. When quadrupole coupling is also included, the cross section at large angle increases slightly and the solid line is obtained. The results of a calculation including only quadrupole coupling are represented by the dotted line. In this case, the interaction couples the entrance channel with both the inelastic and the breakup channels. In this case, the cross section remains appreciable at large angles, indicating that the couplings give rise to a repulsive polarization potential. We point out that the inelastic state is only excited when the quadrupole coupling is included in the calculation. Otherwise, the matrix elements between the elastic and the inelastic channels and between one- and two-phonon states vanish. This is because we are using the first-order harmonic vibrational model to describe the excitation of the target. The dot-dot-dashed line represents the results when only even multipoles are included ($\lambda = 0, \lambda = 2$). Comparing this curve with the long-dashed line, one concludes that the effects of the quadrupole deformations are of the same magnitude as those of the dipole. This conclusion is in agreement with the calculations of Ref. [21], where important interference of first-order $E2$ with second-order $E1$ transitions for populating the p-wave continuum was found.

IV. CONCLUSIONS

We used the CDCC method to evaluate elastic angular distributions for the ^{8}B + ^{58}Ni system at near-barrier energies.

Our results were compared with the recent data of Aguilera *et al.* [12]. The results of our calculations were in excellent agreement with the experimental results.

We have also investigated the effects of inelastic excitations and of continuum-continuum couplings on the angular distributions. We found that inelastic excitations do not have an appreciable influence while continuum-continuum couplings are of utmost importance. We have shown that the multipole expansion of the coupling interaction is dominated by monopole, dipole, and quadrupole terms. Higher multipoles can be neglected.

ACKNOWLEDGMENTS

The authors acknowledge financial support from the CNPq, the FAPERJ, the PRONEX, and the CONACYT.

[1] L. F. Canto, P. R. S. Gomes, R. Donangelo, and M. S. Hussein, Phys. Rep. **424**, 1 (2006).
[2] C. A. Bertulani, M. S. Hussein, and G. Münzenberg, *Physics of Radioactive Beams* (Nova Science, New York, 2001); C. A. Bertulani, L. F. Canto, and M. S. Hussein, Phys. Rep. **226**, 281 (1993).
[3] T. Motobayashi *et al.*, Phys. Rev. Lett. **73**, 2680 (1994); T. Kikuchi *et al.*, Phys. Lett. **B391**, 261 (1997); J. von Schwarzenberg, J. J Kolata, D. Peterson, P. Santi, M. Belbot, and J. D. Hinnefeld, Phys. Rev. C **53**, R2598 (1996).
[4] J. J. Kolata, V. Guimarães, D. Peterson, P. Santi, R. H. White-Stevens, S. M. Vincent, F. D. Becchetti, M. Y. Lee, T. W. O'Donnell, D. A. Roberts, and J. A. Zimmerman, Phys. Rev. C **63**, 024616 (2001).
[5] Y. Sakuragi, M. Yahiro, and M. Kamimura, Prog. Theor. Phys. Suppl. **89**, 136 (1986).
[6] F. M. Nunes and I. J. Thompson, Phys. Rev. C **57**, R2818 (1998).
[7] F. M. Nunes and I. J. Thompson, Phys. Rev. C **59**, 2652 (1999).
[8] J. A. Tostevin, F. M. Nunes, and I. J. Thompson, Phys. Rev. C **63**, 024617 (2001).
[9] H. D. Marta, L. F. Canto, R. Donangelo, and P. Lotti, Phys. Rev. C **66**, 024605 (2002); H. D. Marta, L. F. Canto, and R. Donangelo, *ibid.* **78**, 034612 (2008).
[10] J. Lubian and F. M. Nunes, J. Phys. G: Nucl. Part. Phys. **34**, 513 (2007).
[11] J. Lubian, T. Correa, P. R. S. Gomes, and L. F. Canto, Phys. Rev. C **78**, 064615 (2008).
[12] E. F. Aguilera, E. Martinez-Quiroz, D. Lizcano, A. Gómez-Camacho, J. J. Kolata, L. O. Lamm, V. Guimarães, R. Lichtenthäler, O. Camargo, F. D. Becchetti, H. Jiang, P. A. DeYoung, P. J. Mears, and T. L. Belyaeva, Phys. Rev. C **79**, 021601(R) (2009).
[13] I. J. Thompson, Comput. Phys. Rep. **7**, 167 (1988).
[14] F. D. Becchetti and G. W. Greenlees, Phys. Rev. **182**, 1190 (1969).
[15] H. Esbensen and G. F. Bertch, Nucl. Phys. **A600**, 37 (1996).
[16] L. C. Chamon *et al.*, Nucl. Phys. **A597**, 253 (1996).
[17] Z. Moroz *et al.*, Nucl. Phys. **A381**, 294 (1982).
[18] N. C. Summers, F. M. Nunes, and I. J. Thompson, Phys. Rev. C **74**, 014606 (2006).
[19] A. Diaz-Torres and I. J. Thompson, Phys. Rev. C **65**, 024606 (2002).
[20] A. R. Garcia *et al.*, Phys. Rev. C **76**, 067603 (2007).
[21] J. A. Tostevin, F. M. Nunes, and I. J. Thompson, Phys. Rev. C **63**, 024617 (2001).